NASA Technical Paper 1920

GRID3O – Computer Program for Fast Generation of Multilevel, Three-Dimensional Boundary-Conforming O-Type Computational Grids

Djordje S. Dulikravich

SEPTEMBER 1981

NASA

NASA Technical Paper 1920

GRID3O – Computer Program for Fast Generation of Multilevel, Three-Dimensional Boundary-Conforming O-Type Computational Grids

Djordje S. Dulikravich
Lewis Research Center
Cleveland, Ohio

NASA
National Aeronautics
and Space Administration

Scientific and Technical
Information Branch

1981

Summary

A fast algorithm has been developed for accurately generating boundary-conforming, three-dimensional, consecutively refined computational grids applicable to arbitrary wing-body and axial turbomachinery geometries. The method is based on using an analytic function to generate two-dimensional grids on a number of coaxial axisymmetric surfaces positioned between the centerbody and the outer radial boundary. These grids are of the O-type and are characterized by quasi-orthogonality, geometric periodicity, and an adequate resolution throughout the flow field. Because the built-in nonorthogonal coordinate stretching and shearing cause the grid lines leaving the blade or wing trailing edge to end at downstream infinity, the numerical treatment of the three-dimensional trailing vortex sheets is simplified.

Introduction

When solving partial differential equations governing fluid flow, exact boundary conditions should be applied on all boundaries. This requirement is easily met with a grid generated by the computer program GRID3O, which creates a three-dimensional grid conforming to an irregularly shaped blade (or wing), hub (or fuselage), and duct (or outer radial boundary or wind tunnel wall). Such a boundary-conforming grid is transformed to a parallelepipedal X, Y, Z computational space (fig. 1) in which mesh cells become adjacent cubes and a finite difference discretization of the governing fluid dynamic equations can be performed.

Three-dimensional boundary-conforming grids for cascades of blades (as well as for the single wing-body combination) can be generated by a variety of methods (ref. 1). The method used in the present work has the distinct advantage of being exceptionally fast and easy to understand. It is based on a single conformal mapping function (refs. 2 to 4) and on several additional simple analytical relations that perform coordinate stretchings and shearings. GRID3O also achieves a very high accuracy and a remarkable reliability in the discretized representation of the solid boundaries.

Applicability of the Computer Program

Computer program GRID3O is capable of generating x,y,z or x,θ,r coordinates of a maximum of three consecutively refined boundary-conforming

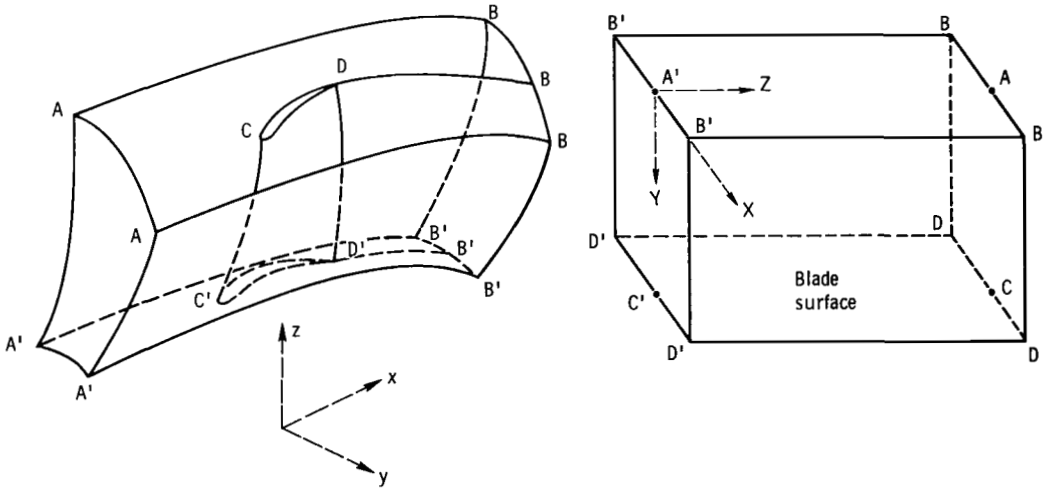

(a) Physical space. (b) Computational space.

Figure 1. - Global geometric transformation.

grids for any of the following three-dimensional configurations:

(1) Arbitrarily shaped wing midmounted on an axisymmetric fuselage: This wing-body combination can be in free air or in a wind tunnel having a doubly infinite axisymmetric wall.

(2) Propeller-type (usually referred to as "horizontal axis") windmill rotor having an arbitrary number of arbitrarily shaped blades mounted on an axisymmetric hub

(3) Helicopter rotor

(4) Propeller (prop-fan) for aircraft propulsion: The propeller can be in free air or in an axisymmetric wind tunnel.

(5) Axial turbomachinery stator

(6) Axial turbomachinery rotor

(7) Ducted fan with rotor diameter smaller than the duct diameter

(8) Propeller for marine propulsion: The propeller can be either free or ducted.

It is important to note that both the hub (or centerbody) and the duct (or wind tunnel wall) can have arbitrary axisymmetric shapes. The number of blades is theoretically arbitrary, although GRID3O has certain limitations, which are explained in the following section. Each blade can be defined by as many as 51 different local airfoil sections. The general blade (or wing) can incorporate an arbitrary spanwise distribution of chord length, thickness, twist angle, sweep angle, and dihedral angle. GRID3O is equally applicable to blades (or wings) with blunt (or rounded), wedged, and cusped trailing and/or leading edges.

Limitations of the Computer Program GRID3O

Computer program GRID3O has several minor limitations. They are the following:

(1) All geometric parameters defining the blade shape must vary smoothly in the spanwise direction.

(2) The hub and shroud are doubly infinite. If the actual hub has a finite length, it must be specified as having thin "stings" extending from the end points toward the axial infinities (fig. 2).

(3) The hub and shroud radii must vary smoothly in the direction of the axis of rotation.

(4) The blade tip chord length must have a nonzero value.

(5) The maximum number of blades is limited by the fact that the minimum local value of the gap-to-chord ratio at any spanwise station must be greater than approximately $(h/c)_{min} \geq 0.65$, where h is the spacing between the blades and c is the local blade chord length. This limiting ratio can be higher if the blade sections are highly staggered. Other factors that can increase $(h/c)_{min}$ are higher airfoil camber and relative thickness. The maximum number of blades NB can be *a priori* estimated as

$$NB \leq 2\pi \left(\frac{r}{c}\right) \frac{1}{(h/c)_{min}}$$

where r is radial distance from the axis of rotation.

(6) The maximum absolute value of the local stagger angle (angle between chord line and meridional plane) for typical axial compressor blades is limited in GRID3O to $|\beta|_{max} \leq 65°$. The value of $|\beta|_{max}$ can be considerably larger ($|\beta|_{max} \approx 90°$) in the outer portions of wind turbine blades or propellers. In an axial gas turbine blade row, $|\beta|_{max}$ will be lower because of the low values of $(h/c)_{min}$ and the high camber and relative thickness (ref. 5).

(7) GRID3O does not allow for the existence of part-span dampers between blades.

(8) Besides blades, hub, and shroud, no other solid boundaries may be present in the flow field.

Grid-Generating Procedure

When analyzing any of the configurations mentioned in the section on applicability (except the wing-body combination), it is sufficient to consider a

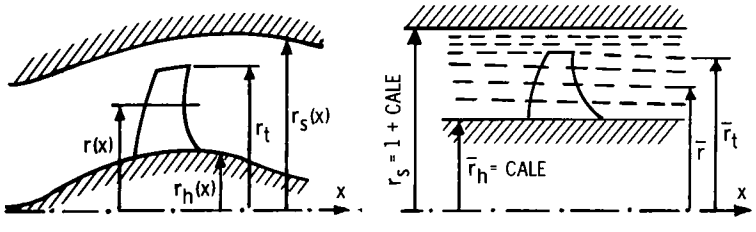

$$\bar{r} = + \frac{r(x) - r_h(x)}{r_s(x) - r_h(x)} + CALE$$

Figure 2. - Radial coordinate normalization.

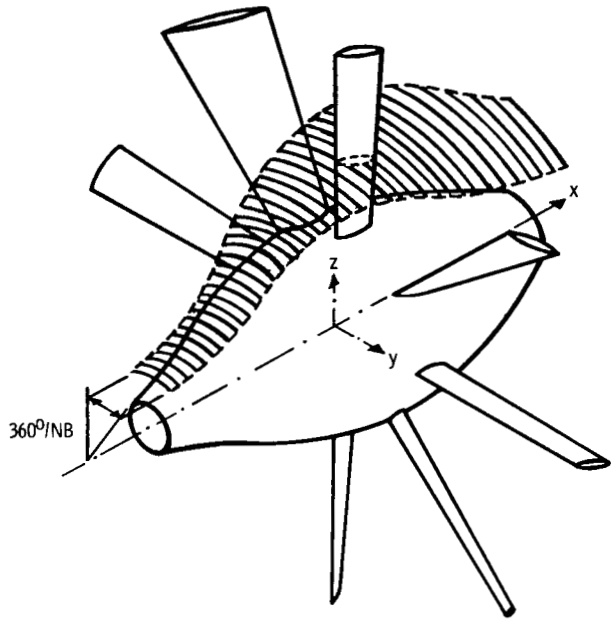

Figure 3. - An axisymmetric cutting surface.

single rotationally periodic segment of the flow field (fig. 3). This segment is a doubly infinite periodic volume stretching in the direction of the axis of rotation. The volume has a constant angular width of 360°/NB, where NB is the total number of blades. The blades have arbitrary spanwise distributions of taper, sweep, dihedral, and twist angles. The local airfoil shapes can vary in an arbitrary fashion along the blade span. The rotor hub and the duct (or shroud) can have different arbitrary axisymmetric shapes. Such an arbitrary three-dimensional physical domain is first discretized in the spanwise direction by a number of coaxial axisymmetric surfaces that are, in general, irregularly spaced between the hub and the shroud. Each of these surfaces is then discretized.

The major problem in generating and discretizing the axisymmetric surfaces is an accurate determination of the intersection contours between the irregular blade surface and the coaxial axisymmetric surfaces cutting the blade. The coordinates of the points on these contours are defined by fitting cubic splines along the blade and interpolating at the radial stations corresponding to each axisymmetric surface, $\bar{r}$ = constant (fig. 2).

Once the shape of the intersection contour on a particular cutting axisymmetric surface is known, the problem becomes one of discretizing a doubly connected two-dimensional domain, $\tilde{w} = x' + i\bar{r}\theta'$ (fig. 4).

Each two-dimensional grid should have the following features:

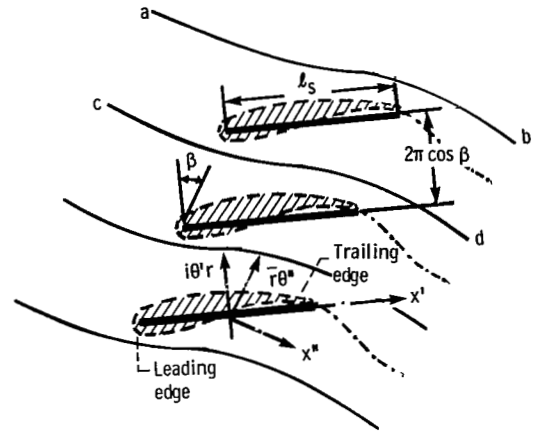

Figure 4. - Two-dimensional axisymmetric surface $\tilde{w}$.

(1) Grid cells should conform to the local contour shape and the shape of the periodic boundaries $\overline{ab}$ and $\overline{cd}$.

(2) Grid should be geometrically periodic in the θ'' direction, meaning that the grid points along the periodic boundary $\overline{ab}$ must have the same respective x'' coordinates (fig. 4) as the grid points along the periodic boundary $\overline{cd}$.

(3) Grid lines should not be excessively nonorthogonal near solid boundaries.

(4) A grid line emanating from the trailing edge should end at downstream infinity.

(5) Grid cells should be concentrated in the regions of high surface curvature.

A grid with these properties can be most easily generated by using a single analytic function. One such function is (ref. 4)

$$\tilde{w} = e^{i\beta} \ln\left(\frac{m - \tilde{z}}{m + \tilde{z}}\right) + e^{-i\beta} \ln\left(\frac{1 - m\tilde{z}}{1 + m\tilde{z}}\right) \quad 0 < m < 1$$

where $\tilde{w} = x' + ir\theta'$ and $\tilde{z} = \xi + i\eta$. This complex function maps conformally a unit circle with a straight slit in the middle (fig. 5) whose end points are situated at $\tilde{z} = \pm m$ onto the cascade of straight slits in the $\tilde{w}$ plane. Each slit has a length l_s, where

$$l_s = 4\left(\cos\beta \sinh^{-1}\frac{2m\cos\beta}{1-m^2} + \sin\beta \sin^{-1}\frac{2m\sin\beta}{1+m^2}\right)$$

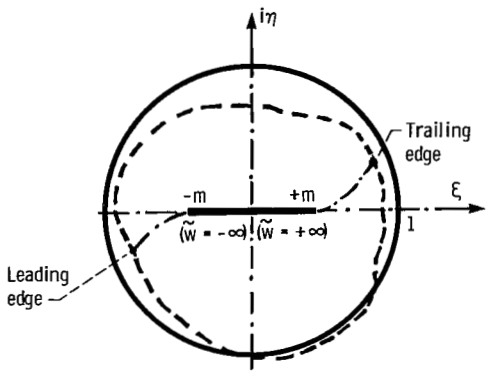

Figure 5. - Conformally mapped periodic strip on $\tilde{z}$-plane.

The slits are spaced $2\pi \cos \beta$ distance apart, where β is the stagger angle of the cascade of slits (fig. 4). The unit circle is "unwrapped" by using elliptic polar coordinates (ref. 6), resulting in a deformed rhomboidal shape that is then sheared in the horizontal and vertical directions to give a rectangular X, Y computational domain.

The transformation of an actual cascade of airfoils will result in a cascade of unit circles that are deformed (fig. 5). Consequently, more nonorthogonality will be introduced in the transformation by additional shearing of coordinates (fig. 6). A uniform grid in the X, Y plane that is symmetrically spaced with respect to the Y axis remaps back into the physical $x'', \bar{r}\theta''$ plane as an O-type boundary-conforming grid (fig. 7). The actual radial coordinates are obtained by fitting cubic splines along the elliptic grid lines and interpolating at a number of axial stations at which the radius of the corresponding axisymmetric surface is known.

A disadvantage of the present method is that it is not applicable for very thick, highly twisted blades that are very closely spaced (fig. 8). This problem can be resolved by using a different form of the mapping function, for example, one that maps a cascade of circles into a cascade of circular arcs instead of a cascade of straight slits.

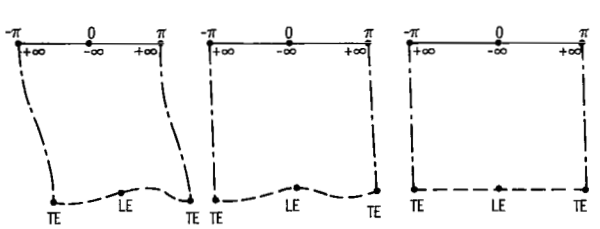

Figure 6. - Nonorthogonal coordinate shearing (where LE denotes leading edge, and TE denotes trailing edge).

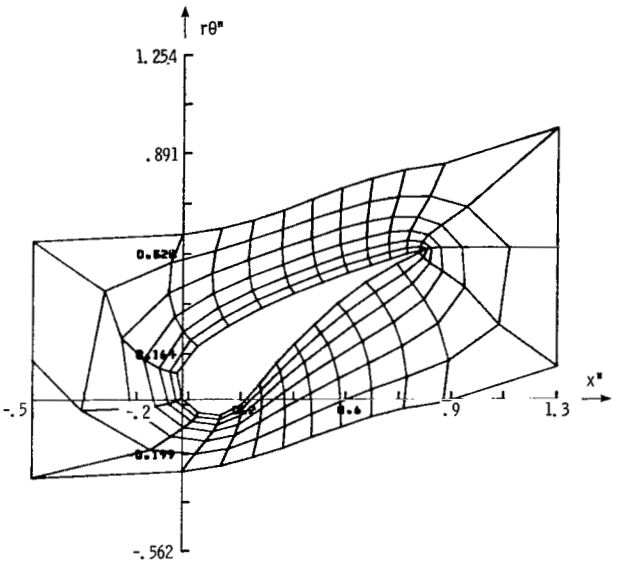

Figure 7. - Example of an O-type grid for a thick airfoil and small gap-chord ratio.

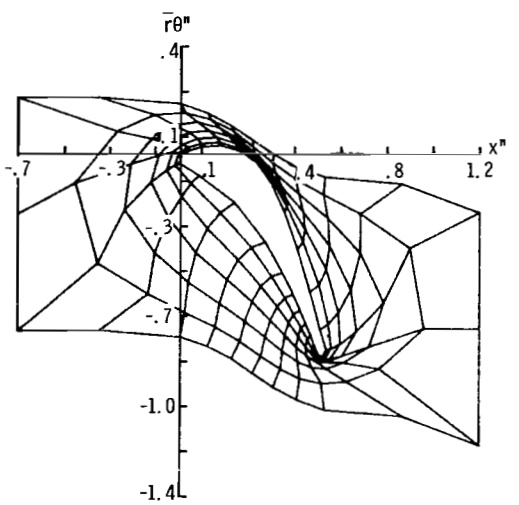

Figure 8. - Grid deformations in the case of closely spaced, thick, highly cambered and staggered blades.

Computer Program

General Description

The computer program GRID3O consists of a main program (fig. 9) and eight subroutines. Input to GRID3O is accomplished by a separate deck of cards, which will be discussed in detail in the following section. Parts of the output from GRID3O appear in standard computer printout form; the major portion of the output (representing

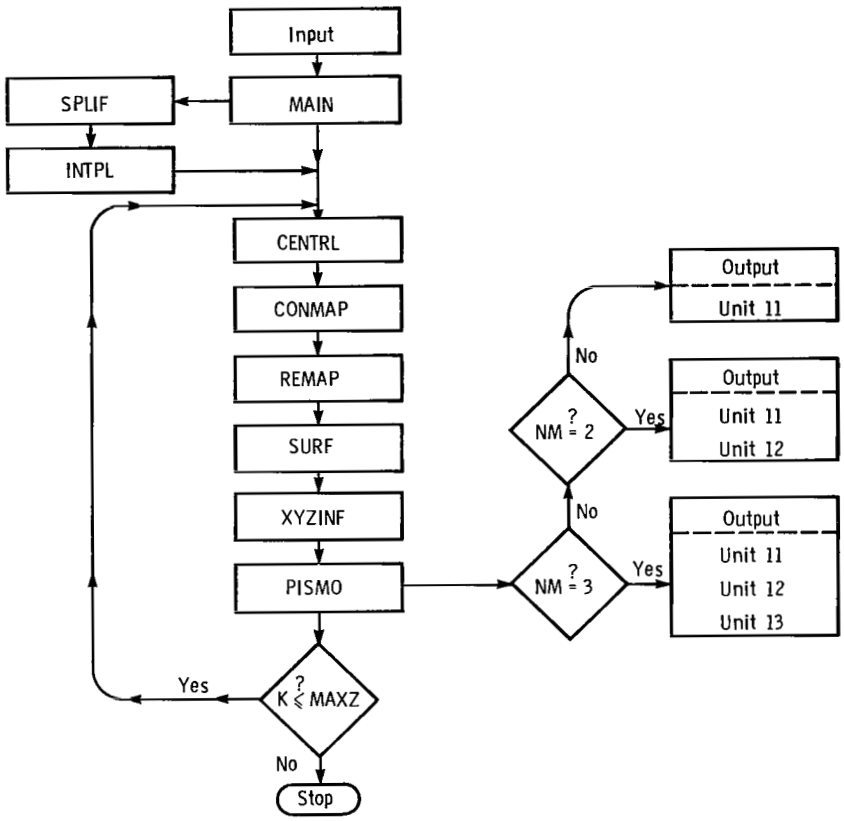

Figure 9. - Flow chart of GRID3O computer program.

coordinates of each grid point) is automatically written on tapes or disks (units 11, 12, and 13).

The main program reads all input data and determines coordinates of the intersection contours created by the axisymmetric computational surfaces and the blade surface (fig. 3). This is performed by fitting cubic splines (subroutine SPLIF) along the blade span and interpolating (subroutine INTPL) at desired radial stations. The intersection contour on each axisymmetric surface is expressed in $x'', \bar{r}\theta''$ coordinates and iteratively mapped by using subroutine CONMAP onto a deformed unit circle (fig. 5). Auxiliary coordinate stretchings and an iterative determination of the slit length in the circle plane are performed by subroutine CENTRL.

CONMAP "unwraps" the circle with the slit in the middle by using an elliptic polar coordinate transformation. The resulting deformed rhomboidal shape is then transformed into a parallelepipedal shape by using nonorthogonal coordinate stretching and shearing in both coordinate directions. Subroutine REMAP maps points (which must be equidistantly spaced with respect to $X=0$) back into the $x'', \bar{r}\theta''$ space.

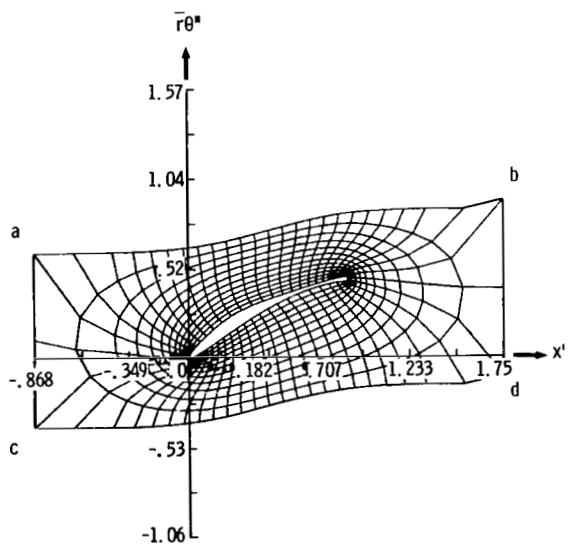

Figure 10. - Example of a two-dimensional grid.

Coordinates of the resulting body-conforming grid (fig. 10) on each $x'', r\theta''$ strip are then interpolated on their respective axisymmetric surface by using subroutine SURF.

For easier numerical application of the boundary conditions at axial infinities the grid has to be suitably shaped at the axial infinity cutoffs. This task is performed by the subroutine XYZINF.

Finally, subroutine PISMO writes x,y,z or x,θ,r coordinates on disks or tapes.

Input

The entire input to GRID3O, in card form, is shown in figure 11. The first card is the title card on which the user can write as many as 80 alphanumerical characters (fig. 12) specifying the name of the input deck. This text will also appear on the output listing from GRID3O.

The second card contains the following 11 input parameters:

```
PENN STATE UNIVERSITY - SUBSONIC DUCTED ROTOR GEOMETRY
KX= 24KY=  6KZ=  6KT=  6NM=  2NH= 10ND= 10NB= 215A=  0.00DZ=  1.0000RT=  0.4661
 -1.000000  0.233100 -1.000000  0.466100
 -0.700000  0.233100 -0.700000  0.466100
 -0.300000  0.233100 -0.300000  0.466100
 -0.000000  0.233100 -0.000000  0.466100
  0.200000  0.233100  0.200000  0.466100
  0.500000  0.233100  0.500000  0.466100
  0.700000  0.233100  0.700000  0.466100
  1.000000  0.233100  1.000000  0.466100
  1.300000  0.233100  1.300000  0.466100
  1.700000  0.233100  1.700000  0.466100
  0.000001  0.233100  0.000000  0.121100  0.006600  0.009900 21.000000  1 43
1.0000000 0.9875000 0.9500000 0.9000000 0.8500000 0.8000000 0.7500000 0.7000000
0.6500000 0.6000000 0.5000000 0.4000000 0.3500000 0.3000000 0.2500000 0.2000000
0.1500000 0.1000000 0.0500000 0.0250000 0.0125000 0.0000000 0.0125000 0.0250000
0.0500000 0.1000000 0.1500000 0.2000000 0.2500000 0.3000000 0.3500000 0.4000000
0.5000000 0.6000000 0.6500000 0.7000000 0.7500000 0.8000000 0.8500000 0.9000000
0.9500000 0.9875000 1.0000000 0.0000000 0.0000000 0.0000000 0.0000000 0.0000000
0.0000000-0.0032000 0.0081000 0.0194000 0.0262000 0.0290000 0.0323000 0.0355000
0.0371000 0.0355000 0.0339000 0.0306000 0.0258000 0.0242000 0.0210000 0.0177000
0.0129000 0.0097000 0.0016000-0.0032000-0.0048000 0.0000000 0.0161000 0.0226000
0.0419000 0.0645000 0.0855000 0.0935000 0.1016000 0.1065000 0.1113000 0.1129000
0.1177000 0.1113000 0.1081000 0.0968000 0.0919000 0.0806000 0.0694000 0.0548000
0.0323000 0.0161000 0.0000000 0.0000000 0.0000000 0.0000000 0.0000000 0.0000000
  0.000001  0.279700  0.000000  0.125600  0.007100  0.010300 24.000000  1 43
1.0000000 0.9875000 0.9500000 0.9000000 0.8500000 0.8000000 0.7500000 0.7000000
0.6500000 0.6000000 0.5000000 0.4000000 0.3500000 0.3000000 0.2500000 0.2000000
0.1500000 0.1000000 0.0500000 0.0250000 0.0125000 0.0000000 0.0125000 0.0250000
0.0500000 0.1000000 0.1500000 0.2000000 0.2500000 0.3000000 0.3500000 0.4000000
0.5000000 0.6000000 0.6500000 0.7000000 0.7500000 0.8000000 0.8500000 0.9000000
0.9500000 0.9875000 1.0000000 0.0000000 0.0000000 0.0000000 0.0000000 0.0000000
0.0000000-0.0032000 0.0143000 0.0238000 0.0317000 0.0381000 0.0413000 0.0429000
0.0444000 0.0444000 0.0397000 0.0349000 0.0333000 0.0317000 0.0286000 0.0238000
0.0190000 0.0095000 0.0063000 0.0032000-0.0016000 0.0000000 0.0206000 0.0302000
0.0429000 0.0651000 0.0794000 0.0937000 0.1016000 0.1095000 0.1159000 0.1190000
0.1190000 0.1143000 0.1063000 0.1000000 0.0905000 0.0794000 0.0683000 0.0540000
0.0381000 0.0190000 0.0000000 0.0000000 0.0000000 0.0000000 0.0000000 0.0000000
  0.000001  0.326300  0.000000  0.130100  0.007000  0.010000 28.000000  1 43
1.0000000 0.9875000 0.9500000 0.9000000 0.8500000 0.8000000 0.7500000 0.7000000
0.6500000 0.6000000 0.5000000 0.4000000 0.3500000 0.3000000 0.2500000 0.2000000
0.1500000 0.1000000 0.0500000 0.0250000 0.0125000 0.0000000 0.0125000 0.0250000
0.0500000 0.1000000 0.1500000 0.2000000 0.2500000 0.3000000 0.3500000 0.4000000
0.5000000 0.6000000 0.6500000 0.7000000 0.7500000 0.8000000 0.8500000 0.9000000
0.9500000 0.9875000 1.0000000 0.0000000 0.0000000 0.0000000 0.0000000 0.0000000
0.0000000-0.0062000 0.0092000 0.0215000 0.0308000 0.0354000 0.0415000 0.0446000
0.0462000 0.0462000 0.0462000 0.0431000 0.0400000 0.0369000 0.0338000 0.0292000
0.0231000 0.0169000 0.0077000 0.0015000-0.0031000 0.0000000 0.0200000 0.0292000
0.0415000 0.0662000 0.0800000 0.0923000 0.1000000 0.1076000 0.1138000 0.1169000
0.1169000 0.1108000 0.1031000 0.0954000 0.0846000 0.0754000 0.0615000 0.0477000
0.0292000 0.0138000 0.0000000 0.0000000 0.0000000 0.0000000 0.0000000 0.0000000
  0.000001  0.373000  0.000000  0.135300  0.007400  0.010300 32.000000  1 43
1.0000000 0.9875000 0.9500000 0.9000000 0.8500000 0.8000000 0.7500000 0.7000000
0.6500000 0.6000000 0.5000000 0.4000000 0.3500000 0.3000000 0.2500000 0.2000000
0.1500000 0.1000000 0.0500000 0.0250000 0.0125000 0.0000000 0.0125000 0.0250000
0.0500000 0.1000000 0.1500000 0.2000000 0.2500000 0.3000000 0.3500000 0.4000000
0.5000000 0.6000000 0.6500000 0.7000000 0.7500000 0.8000000 0.8500000 0.9000000
0.9500000 0.9875000 1.0000000 0.0000000 0.0000000 0.0000000 0.0000000 0.0000000
0.0000000-0.0016000 0.0148000 0.0279000 0.0361000 0.0426000 0.0459000 0.0492000
0.0525000 0.0525000 0.0492000 0.0475000 0.0459000 0.0426000 0.0377000 0.0328000
0.0279000 0.0213000 0.0098000 0.0049000 0.0053000 0.0000000 0.0131000 0.0230000
0.0361000 0.0590000 0.0738000 0.0836000 0.0918000 0.0984000 0.1049000 0.1082000
0.1082000 0.1016000 0.0967000 0.0902000 0.0820000 0.0738000 0.0639000 0.0492000
0.0311000 0.0148000 0.0000000 0.0000000 0.0000000 0.0000000 0.0000000 0.0000000
  0.000001  0.419600  0.000000  0.141400  0.007100  0.009900 38.000000  1 43
1.0000000 0.9875000 0.9500000 0.9000000 0.8500000 0.8000000 0.7500000 0.7000000
0.6500000 0.6000000 0.5000000 0.4000000 0.3500000 0.3000000 0.2500000 0.2000000
0.1500000 0.1000000 0.0500000 0.0250000 0.0125000 0.0000000 0.0125000 0.0250000
0.0500000 0.1000000 0.1500000 0.2000000 0.2500000 0.3000000 0.3500000 0.4000000
0.5000000 0.6000000 0.6500000 0.7000000 0.7500000 0.8000000 0.8500000 0.9000000
0.9500000 0.9875000 1.0000000 0.0000000 0.0000000 0.0000000 0.0000000 0.0000000
0.0000000-0.0014000 0.0125000 0.0264000 0.0361000 0.0458000 0.0514000 0.0562000
0.0556000 0.0597000 0.0597000 0.0556000 0.0562000 0.0486000 0.0444000 0.0403000
0.0349000 0.0250000 0.0153000 0.0083000 0.0014000 0.0000000 0.0181000 0.0264000
0.0419000 0.0583000 0.0764000 0.0889000 0.0972000 0.1042000 0.1097000 0.1139000
0.1153000 0.1069000 0.1000000 0.0903000 0.0833000 0.0750000 0.0611000 0.0472000
0.0153000 0.0111000 0.0000000 0.0000000 0.0000000 0.0000000 0.0000000 0.0000000
  0.000001  0.466100  0.000000  0.150400  0.006600  0.010000 45.000000  3 43
1.0000000 0.9875000 0.9500000 0.9000000 0.8500000 0.8000000 0.7500000 0.7000000
0.6500000 0.6000000 0.5000000 0.4000000 0.3500000 0.3000000 0.2500000 0.2000000
0.1500000 0.1000000 0.0500000 0.0250000 0.0125000 0.0000000 0.0125000 0.0250000
0.0500000 0.1000000 0.1500000 0.2000000 0.2500000 0.3000000 0.3500000 0.4000000
0.5000000 0.6000000 0.6500000 0.7000000 0.7500000 0.8000000 0.8500000 0.9000000
0.9500000 0.9875000 1.0000000 0.0000000 0.0000000 0.0000000 0.0000000 0.0000000
0.0000000-0.0016000 0.0159000 0.0254000 0.0349000 0.0413000 0.0460000 0.0476000
0.0524000 0.0508000 0.0508000 0.0460000 0.0444000 0.0413000 0.0381000 0.0317000
0.0270000 0.0206000 0.0095000 0.0032000 0.0008000 0.0000000 0.0127000 0.0206000
0.0302000 0.0508000 0.0651000 0.0730000 0.0841000 0.0889000 0.0937000 0.0952000
0.0968000 0.0921000 0.0887000 0.0825000 0.0746000 0.0667000 0.0571000 0.0460000
0.0968000 0.0921000 0.0887000 0.0825000 0.0746000 0.0667000 0.0571000 0.0460000
0.0968000 0.0921000 0.0887000 0.0825000 0.0746000 0.0667000 0.0571000 0.0460000
```

Figure 11. - Example of an input deck for a blade composed from several different input airfoil shapes.

Card	Format
1	TITLE
	20A4
2	KX, KY, KZ, KT, NM, NH, ND, NB, SA, DZ, RT
	8 (3X, I3); 3X, F6.2, 3X, F8.4, 3X, F8.4
3 to m	XHUB (I), RHUB (I), XDUCT (I), RDUCT (I)
	4F10.6
m + 1	XLEAD, ZLEAD, YLEAD, CHORD, RO1, RO2, TWIST, NF, MAXP, N
	7F10.6, 3I3
(m + 2) to n	x' (1), . . . , x' (8)
	8F10.7
n + 1	y' (1), . . . , y' (8)
	Same as m + 1
.	.
.	.
.	.

Figure 12. - Input format for GRID3O computer program.

KX number of grid cells around the blade, that is, the number of grid cells on the first (coarse) grid in the direction of the computational X axis. Suggested value is KX = 24. Users of GRID3O should remember that KX must be an even number.

KY number of grid cells in the computational Y direction, that is, the number of elliptic (wraparound) layers of grid cells around the blade on the first (coarse) grid. Suggested value is KY = 6. It is advisable to specify the value of KY from the following relation:

$$KY = KX/4$$

KZ number of grid cells in the spanwise direction (computational Z direction) from the hub to the outer radial boundary (fig. 2) on the first (coarse) grid. The shape and radial distance of the outer boundary surface will be specified later in the input.

KT number of grid cells in the spanwise direction from hub to tip on the first (coarse) grid. The minimum value of KZ must be

$$KZ \geq KT + 3$$

KT is equal to KZ only when r_t is equal to the radius of the outer boundary, where r_t is the rotor radius. The blade tip will be in the middle of the $(KT + 1)^{th}$ grid cell except in the case where KT = KZ. Then the blade tip will be touching the shroud (duct) wall.

NM number of grid refinements. If NM = 1, only the coarse three-dimensional grid consisting of (KX•KY•KZ) grid cells will be generated and its x,y,z (or x,θ,r) coordinates permanently stored on unit 11. If NM = 2, this coarse grid will be refined by doubling the number of grid cells in each of three computational directions. Coordinates of this refined (second) grid will then be automatically written on unit 12, but the coordinates of the coarse (first) grid will remain stored on unit 11. If NM = 3 on the second input card, the second grid will also be refined in the same manner as was the first grid. The coordinates of this fine (third) grid will then be written on unit 13. Users of GRID3O should be aware of the computer storage requirements resulting from the successive grid refinement procedure (fig. 13). The present version of GRID3O is capable of automatically generating coordinates for as many as three (NM = 3) refined grids, the third grid having a maximum of $192 \times 48 \times 48$ grid cells. These values can be changed by changing COMMON and DIMENSION statements. If

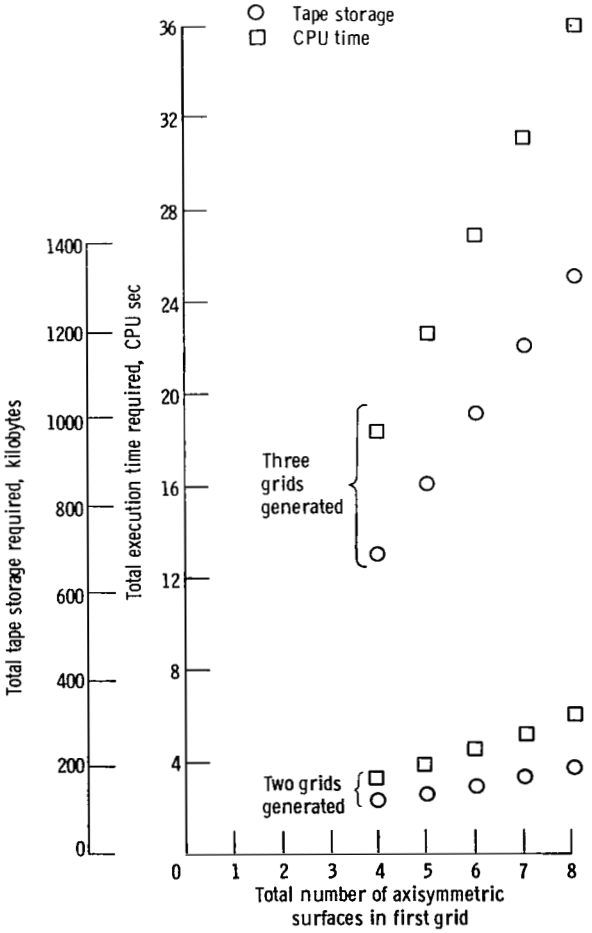

Figure 13. - Computer requirements and GRID3O performance chart.

NM is given a negative sign, output from GRID3O program will be x,θ,r coordinates.

NH number of input points defining hub and sting surface. The maximum value for NH is 51.

ND number of input points defining duct (or outer radial boundary) surface. The maximum value for ND is 51. ND must be equal to or less than NH.

NB number of blades. The minimum value for NB is 2.

SA setting (pitch) angle of the blade, deg. SA represents the constant angle that will be automatically added to the local stagger (twist) angle at each spanwise input station. When generating a sequence of grids for a variable-pitch rotor (or stator), it is necessary each time to change the value of SA only; the rest of the input should stay the same.

DZ length scaling coefficient. DZ multiplies all output length parameters generated by GRID3O program.

Input length units	Output length units	DZ
meters	meters	1.000
feet	feet	1.000
feet	meters	0.3048
meters	feet	3.2808

RT rotor radius, or wing half span.

A number of the following input cards (card 3 to card m in fig. 12) specify hub and shroud geometry. Each of these input cards lists the following values:

x_h x coordinate of the input point on the hub or sting surface

r_h r coordinate of the input point on the hub or sting surface

x_s x coordinate of the input point on the outer radial boundary

r_s r coordinate of the input point on the outer radial boundary

Hub and shroud surfaces should be defined at least 10 chord lengths upstream and downstream of the rotor.

In a turbomachinery stator, rotor, or ducted fan the outer radial boundary represents the surface of a duct or shroud. In the remaining text this surface is referred to as a shroud. In a free propeller, a helicopter rotor in hover, or a wing-body combination the outer radial boundary represents an arbitrarily axisymmetrically shaped surface positioned off the blade tip.

Blade geometry is defined on NP parallel input planes (fig. 14), where the first input plane ($N=1$)

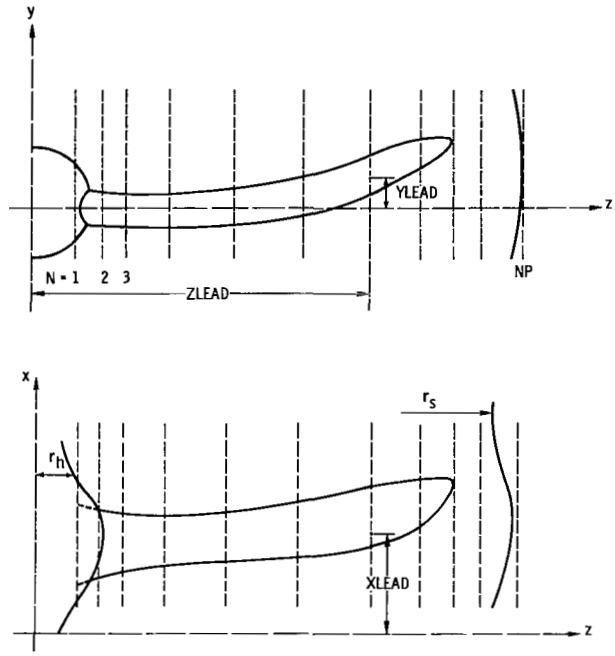

Figure 14. - Spanwise input planes parallel to each other and orthogonal on the z (stacking) axis.

must be entirely inside the hub and the last input plane must be entirely at or beyond the shroud surface or outer radial boundary surface.

The following input card (card $m+1$ in fig. 12) contains geometric parameters specifying the first spanwise input plane ($N=1$). These parameters are

XLEAD x coordinate of the blade leading edge on the N^{th} input plane (fig. 14). The origin of the x,r,θ coordinate system is arbitrarily positioned on the x axis. Blade stacking axis corresponds to z axis (or r axis).

ZLEAD z coordinate of the blade leading edge on the N^{th} input plane (fig. 15)

YLEAD y coordinate of the blade leading edge on the N^{th} input plane (fig. 14).

CHORD chord length (not the projected chord length) of the blade on the N^{th} input plane (fig. 15)

R01,R02 radii of the blade leading and trailing edges, respectively, on the N^{th} input plane (fig. 15). R01 and R02 must be nondimensionalized with respect to CHORD.

TWIST angle between the blade chord on the N^{th} input plane and the X axis (fig. 15), deg

NF input parameter that indicates if a single airfoil shape was used for the blade design. If NF = 0, the airfoil shape on the

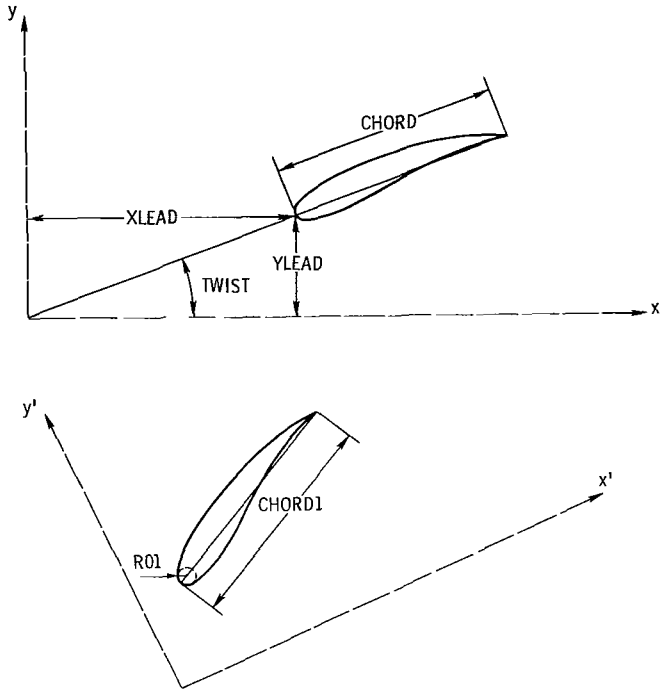

Figure 15. - Input coordinate system on each N^{th} input plane (z = ZLEAD) orthogonal on the z (stacking) axis.

$(N+1)^{th}$ input plane is the same as it was on the N^{th} input plane. If NF = 1, the airfoil shape on the $(N+1)^{th}$ input plane is different (fig. 11) from the airfoil shape on the N^{th} input plane. If NF = 2, this input plane is the last input plane, and the local airfoil shape is the same as on the previous input plane. If NF = 3, the input plane is the last input plane and the local airfoil shape is not the same as on the previous plane.

MAXP number of input points defining airfoil shape on N^{th} input plane. The input points are given in the clockwise direction (fig. 15) starting from the trailing-edge point. If the airfoil shape is nonsymmetric, MAXP must be an odd number (counting the trailing-edge point twice). If the airfoil shape is symmetric, MAXP must be an even number, and only coordinates of points on the lower surface of the airfoil must be specified. The value of MAXP can vary from one N^{th} plane to the next. Maximum number is MAXP = 165.

The following set of input cards (card $m+2$ to card n in fig. 12) specifies the x' and y' input coordinates (fig. 15) defining the airfoil shape on the N^{th} input plane. The origin of the x',y' coordinate system is arbitrarily positioned with respect to the airfoil leading edge (fig. 15). The input coordinates x' and y' do not have to be normalized with respect to the chord length. Scalings and rotation of the input coordinates will be performed automatically by the GRID3O program. The coordinate axis x' does not have to be parallel with the x coordinate axis, but it must be in the N^{th} input plane (fig. 15).

All the x' coordinates are specified in the input separately, followed by all the y' coordinates (fig. 11). The number of x' (or y') coordinates that can be specified on each input card is eight (fig. 12). If the total number of input points (MAXP) is not a multiple of eight, the last input card of a set specifying x' coordinates (as well as the last card specifying y' coordinates) should be filled with the values $x' = 0$ (or $y' = 0$).

This concludes all the input data needed for the N^{th} input plane.

The $(N+1)^{th}$ input plane and the airfoil shape are defined on the following set of input cards, starting with card $n+1$ in figure 12. These cards are identically formatted as are the cards from $m+1$ to n (fig. 12). If NF = 0 or NF = 2 on card $m+1$, the $(N+1)^{th}$ input plane will be defined by a single input card having the format of card $m+1$, as can be seen in figure 16.

Output

Parts of the output of GRID3O will appear in printed form and require approximately two pages of computer printout (fig. 17). The main results of GRID3O are coordinates of three-dimensional body-conforming grids (or grid, if NM = 1). The coordinates of the coarse (first) grid will be automatically written on tape (or disk) 11. If NM = 2 in the input data, coordinates of the second (refined) grid will be written on unit 12; and if NM = 3, the coordinates of the third (fine) grid will be written on unit 13. This storage arrangement provides the user with an opportunity to display and analyze each grid separately. All the WRITE statements are unformatted and can be found in subroutine PISMO.

The output listing specifies the data contained on the first m input cards as well as each $(m+1)^{th}$ card. This serves for easier detecting of errors that may have been made during the preparation of the input.

The output from GRID3O continues with a listing of the following parameters defining airfoil shapes on each of the K computational axisymmetric surfaces.

```
NON-LIFTING SWEPT ONERA WING MID-MOUNTED ON CYLINDRICAL FUSELAGE
KX= 24KY=  6KZ=  8KT=  5NM=  3NH= 10ND= 10NB=  2SA=  0.00DZ=  1.0000RT=  1.2500
 -9.000000  0.250000 -9.000000  3.250000
 -2.500000  0.250000 -2.500000  3.250000
 -1.000000  0.250000 -1.000000  3.250000
 -0.400000  0.250000 -0.400000  3.250000
  0.000000  0.250000  0.000000  3.250000
  0.200000  0.250000  0.200000  3.250000
  0.500000  0.250000  0.500000  3.250000
  1.000000  0.250000  1.000000  3.250000
  2.500000  0.250000  2.500000  3.250000
 12.500000  0.250000 12.500000  3.250000
 -0.057600  0.150000  0.000000  0.703100  0.022000  0.000100  0.000000  1 48
 1.0000000 0.9952000 0.9843000 0.9662000 0.9363000 0.8868000 0.8175000 0.7708000
 0.7232000 0.6753000 0.6268000 0.5778000 0.5282000 0.4781000 0.4274000 0.3761000
 0.3243000 0.2718000 0.2453000 0.2187000 0.1919000 0.1650000 0.1379000 0.1150000
 0.0956000 0.0793000 0.0656000 0.0541000 0.0445000 0.0364000 0.0297000 0.0241000
 0.0195000 0.0156000 0.0124000 0.0098000 0.0077000 0.0060000 0.0046000 0.0034000
 0.0025000 0.0018000 0.0013000 0.0009000 0.0006000 0.0003000 0.0002000 0.0000000
-0.0000000-0.0013000-0.0027000-0.0049000-0.0086000-0.0145000-0.0220000-0.0266000
-0.0309000-0.0350000-0.0388000-0.0422000-0.0450000-0.0472000-0.0485000-0.0489000
-0.0485000-0.0472000-0.0462000-0.0451000-0.0436000-0.0419000-0.0399000-0.0378000
-0.0358000-0.0338000-0.0320000-0.0303000-0.0288000-0.0273000-0.0258000-0.0242000
-0.0225000-0.0206000-0.0188000-0.0169000-0.0151000-0.0134000-0.0117000-0.0102000
-0.0086000-0.0075000-0.0063000-0.0051000-0.0041000-0.0031000-0.0023000 0.0000000
  0.000001  0.250000  0.000000  0.673700  0.022000  0.000100  0.000000  0 48
  0.115000  0.450000  0.000000  0.614800  0.022000  0.000100  0.000000  0 48
  0.230000  0.650000  0.000000  0.555800  0.022000  0.000100  0.000000  0 48
  0.460000  1.050000  0.000000  0.437900  0.022000  0.000100  0.000000  0 48
  0.575000  1.250000  0.000000  0.378900  0.022000  0.000100  0.000000  0 48
  0.600000  2.000000  0.000000  0.320000  0.022000  0.000100  0.000000  0 48
  0.550000  3.250000  0.000000  0.380000  0.022000  0.000100  0.000000  2 48
```

Figure 16. - Example of an input deck for a wing composed from a single air foil shape.

XLEAD x coordinate of blade leading edge on N^{th} surface

ZLEAD z coordinate of blade leading edge on N^{th} surface

YLEAD y coordinate of blade leading edge on N^{th} surface

CHORD chord length of blade (side projection on x-z plane) on K^{th} surface

$$\text{CHORD} = [(y_{TE} - y_{LE})^2 + (x_{TE} - x_{LE})^2]^{1/2}$$

R01,R02 radii of blade leading and trailing edges, respectively, on K^{th} surface

TWIST angle between blade chord on K^{th} surface (side projection on x-z plane) and axis of rotation, deg

$$\text{TWIST} = \sin^{-1}[(y_{TE} - y_{LE})/\text{CHORD}]$$

K label (index) number of particular computational axisymmetric surface generated by GRID3O. The parameter K varies from K = 2 (hub surface) to K = KZ*NM + 2 corresponding to the shroud or outer radial boundary surface

Thus the total number of axisymmetric computational surfaces that will be generated and in a discretized form stored on, for example, tape 13 is

$$\text{MAXZM} = \text{KZ}*3 + 1$$

Because GRID3O automatically generates a layer of imaginary points inside the blade (J = MAXYP) as well as one layer of points off the periodicity (fig. 10) boundaries (J = 2), the total number of layers of points generated on each K^{th} axisymmetric surface is

$$\text{MAXYP} = \text{KY}*\text{NM} + 3$$

Similarly, GRID3O generates double-valued points on the vortex sheet (I = 2 and I = MAXX) trailing from the blade trailing edge (fig. 10). GRID3O also generates two lines (I = 1 and I = MAXXP) of points off the vortex sheet. Hence the total number of lines of points generated on each K^{th} axisymmetric surface is

$$\text{MAXXP} = \text{KX}*\text{NM} + 3$$

As a consequence, tape 11 will contain coordinates of (KX + 3)*(KY + 3)*(KZ + 1) grid points, tape 12 will contain coordinates of (KX*2 + 3)*(KY*2 + 3)*(KZ*2 + 1) grid points, and tape 13 will contain coordinates of (KX*3 + 3)*(KY*3 + 3)*(KZ*3 + 1) grid points. They are all written on these tapes in a single-precision unformatted form.

Lewis Research Center
National Aeronautics and Space Administration
Cleveland, Ohio, February 12, 1981

```
(GRID3D) DEVELOPED BY: DJORDJE S. DULIKRAVICH
NATIONAL RESEARCH COUNCIL-NASA LEWIS CFM BRANCH

3-D MULTILEVEL BOUNDARY-CONFORMING GRID GENERATION

INPUT PARAMETERS

NON-LIFTING SWEPT ONERA WING MID-MOUNTED ON CYLINDRICAL FUSELAGE
  KX      KY      KZ      KT      NM      NB      SA      DZ      RT
  24       6       8       5       3       2    0.00  1.0000  1.2500

      XHUB(I)          RHUB(I)          XDUCT(I)          RDUCT(I)          I
-0.900000E 01    0.250000E 00    -0.900000E 01    0.325000E 01          1
-0.250000E 01    0.250000E 00    -0.250000E 01    0.325000E 01          2
-0.100000E 01    0.250000E 00    -0.100000E 01    0.325000E 01          3
-0.400000E 00    0.250000E 00    -0.400000E 00    0.325000E 01          4
    0.000000     0.250000E 00        0.000000     0.325000E 01          5
 0.200000E 00    0.250000E 00     0.200000E 00    0.325000E 01          6
 0.500000E 00    0.250000E 00     0.500000E 00    0.325000E 01          7
 0.100000E 01    0.250000E 00     0.100000E 01    0.325000E 01          8
 0.250000E 01    0.250000E 00     0.250000E 01    0.325000E 01          9
 0.125000E 02    0.250000E 00     0.125000E 02    0.325000E 01         10

    XLEAD          ZLEAD          YLEAD          CHORD          RO1     RO2    TWIST   N
-0.576000E-01  0.150000E 00     0.000000  0.703100E 00  0.0220  0.0001  0.000   1
 0.100000E-05  0.250000E 00     0.000000  0.673700E 00  0.0220  0.0001  0.000   2
 0.115000E 00  0.450000E 00     0.000000  0.614800E 00  0.0220  0.0001  0.000   3
 0.230000E 00  0.650000E 00     0.000000  0.555800E 00  0.0220  0.0001  0.000   4
 0.460000E 00  0.105000E 01     0.000000  0.437900E 00  0.0220  0.0001  0.000   5
 0.575000E 00  0.125000E 01     0.000000  0.378900E 00  0.0220  0.0001  0.000   6
 0.600000E 00  0.200000E 01     0.000000  0.320000E 00  0.0220  0.0001  0.000   7
 0.550000E 00  0.325000E 01     0.000000  0.380000E 00  0.0220  0.0001  0.000   8

OUTPUT PARAMETERS

    XLEAD          ZLEAD          YLEAD          CHORD          RO1     RO2    TWIST   K
 0.103933E-05  0.250000E 00  0.357791E-15  0.673700E 00  0.0220  0.0001 -0.000   2
 0.280192E-01  0.298750E 00  0.452050E-15  0.659366E 00  0.0220  0.0001 -0.000   3
 0.560240E-01  0.347500E 00  0.540467E-15  0.645024E 00  0.0220  0.0001 -0.000   4
 0.840463E-01  0.396250E 00  0.606847E-15  0.630664E 00  0.0220  0.0001 -0.000   5
 0.112117E 00  0.445000E 00  0.684679E-15  0.616277E 00  0.0220  0.0001 -0.000   6
 0.140252E 00  0.493750E 00  0.762941E-15  0.601860E 00  0.0220  0.0001 -0.000   7
 0.168390E 00  0.542500E 00  0.841634E-15  0.587438E 00  0.0220  0.0001 -0.000   8
 0.196440E 00  0.591250E 00  0.984585E-15  0.573048E 00  0.0220  0.0001 -0.000   9
 0.224313E 00  0.640000E 00  0.105035E-14  0.558726E 00  0.0220  0.0001 -0.000  10
 0.251937E 00  0.688750E 00  0.114969E-14  0.544501E 00  0.0220  0.0001 -0.000  11
 0.279383E 00  0.737500E 00  0.114132E-14  0.530348E 00  0.0220  0.0001 -0.000  12
 0.306785E 00  0.786250E 00  0.122066E-14  0.516215E 00  0.0220  0.0001 -0.000  13
 0.334276E 00  0.835000E 00  0.130020E-14  0.502051E 00  0.0220  0.0001 -0.000  14
 0.361990E 00  0.883750E 00  0.137992E-14  0.487804E 00  0.0220  0.0001 -0.000  15
 0.390062E 00  0.932500E 00  0.154229E-14  0.473423E 00  0.0220  0.0001 -0.000  16
 0.418625E 00  0.981250E 00  0.168793E-14  0.458857E 00  0.0220  0.0001 -0.000  17
 0.447813E 00  0.103000E 01  0.172835E-14  0.444053E 00  0.0220  0.0001 -0.000  18
 0.477714E 00  0.107875E 01  0.176686E-14  0.428980E 00  0.0220  0.0001 -0.000  19
 0.507675E 00  0.112750E 01  0.216511E-14  0.413880E 00  0.0220  0.0001 -0.000  20
 0.536463E 00  0.117625E 01  0.183866E-14  0.399215E 00  0.0220  0.0001 -0.000  21
 0.562827E 00  0.122500E 01  0.187216E-14  0.385454E 00  0.0220  0.0001 -0.000  22
 0.586073E 00  0.127500E 01  0.190500E-14  0.372757E 00  0.0220  0.0001 -0.000  23
 0.604559E 00  0.132375E 01  0.232344E-14  0.361948E 00  0.0220  0.0001 -0.000  24
 0.630363E 00  0.142164E 01  0.239259E-14  0.344570E 00  0.0220  0.0001 -0.000  25
 0.643758E 00  0.152880E 01  0.246197E-14  0.331385E 00  0.0220  0.0001 -0.000  26
 0.644015E 00  0.165360E 01  0.295857E-14  0.322385E 00  0.0220  0.0001 -0.000  27
 0.629568E 00  0.180268E 01  0.305071E-14  0.318415E 00  0.0220  0.0001 -0.000  28
 0.602980E 00  0.198030E 01  0.314814E-14  0.319652E 00  0.0220  0.0001 -0.000  29
 0.574957E 00  0.218793E 01  0.371248E-14  0.324261E 00  0.0220  0.0001 -0.000  30
 0.552281E 00  0.242410E 01  0.382527E-14  0.332005E 00  0.0220  0.0001 -0.000  31
 0.538631E 00  0.268455E 01  0.442468E-14  0.343629E 00  0.0220  0.0001 -0.000  32
 0.537206E 00  0.296264E 01  0.504035E-14  0.359611E 00  0.0220  0.0001 -0.000  33
 0.550000E 00  0.325000E 01  0.566640E-14  0.380001E 00  0.0220  0.0001 -0.000  34
```

Figure 17. - Example of an output listing.

References

1. Numerical Grid Generation Techniques. NASA CP-2166, 1980.
2. Dulikravich, D. S.: Numerical Calculation of Inviscid Transonic Flow Through Rotors and Fans. Ph.D. Thesis, Cornell University, Jan. 1979. (Available through Univ. Microfilms Order No. 7910741, 300 N. Zeeb Rd., Ann Arbor, Michigan 48106.)
3. Dulikravich, D. S.: CAS2D—Fortran Program for Nonrotating Blade-to-Blade, Steady, Potential Transonic Cascade Flows. NASA TP-1705, 1980.
4. Kober, H.: Dictionary of Conformal Representations. Second ed. Dover Publications, Inc., 1957, p. 131.
5. Vavra, M. H.: Aero-Thermodynamics and Flow in Turbomachines. John Wiley & Sons, Inc., 1960, pp. 122-125.
6. Spiegel, M. R.: Mathematical Handbook of Formulas and Tables. Schaum's Outline Series, McGraw-Hill Book Co., Inc., 1968, p. 127.

1. Report No. NASA TP-1920	2. Government Accession No.	3. Recipient's Catalog No.
4. Title and Subtitle GRID3O - COMPUTER PROGRAM FOR FAST GENERATION OF MULTILEVEL, THREE-DIMENSIONAL BOUNDARY-CONFORMING O-TYPE COMPUTATIONAL GRIDS		5. Report Date September 1981 6. Performing Organization Code 505-32-52
7. Author(s) Djordje S. Dulikravich		8. Performing Organization Report No. E-590
9. Performing Organization Name and Address National Aeronautics and Space Administration Lewis Research Center Cleveland, Ohio 44135		10. Work Unit No. 11. Contract or Grant No.
12. Sponsoring Agency Name and Address National Aeronautics and Space Administration Washington, D.C. 20546		13. Type of Report and Period Covered Technical Paper 14. Sponsoring Agency Code

15. Supplementary Notes
The author is a National Research Council - NASA Research Associate at the Lewis Research Center.

16. Abstract

A fast algorithm has been developed for accurately generating boundary-conforming, three-dimensional, consecutively refined computational grids applicable to arbitrary wing-body and axial turbomachinery geometries. The method is based on using an analytic function to generate two-dimensional grids on a number of coaxial axisymmetric surfaces positioned between the centerbody and the outer radial boundary. These grids are of the O-type and are characterized by quasi-orthogonality, geometric periodicity, and an adequate resolution throughout the flow field. Because the built-in nonorthogonal coordinate stretching and shearing cause the grid lines leaving the blade or wing trailing edge to end at downstream infinity, the numerical treatment of the three-dimensional trailing vortex sheets is simplified.

17. Key Words (Suggested by Author(s))	18. Distribution Statement
Grid generation Computational grids Numerical methods Conformal mapping Turbomachinery Geometry	Unclassified - unlimited STAR Category 02

19. Security Classif. (of this report)	20. Security Classif. (of this page)	21. No. of Pages	22. Price*
Unclassified	Unclassified	13	A02

* For sale by the National Technical Information Service, Springfield, Virginia 22161

NASA-Langley, 1981

2 1 1U,A, 090181 S00903DS
DEPT OF THE AIR FORCE
AF WEAPONS LABORATORY
ATTN: TECHNICAL LIBRARY (SUL)
KIRTLAND AFB NM 87117